



# ESO Colloquium (Santiago de Chile)



An E-ELT DRM science case:  
stellar population and stellar dynamics  
in deeply embedded dense massive protoclusters

Hans Zinnecker (AIP and ESO visiting scientist)

OR

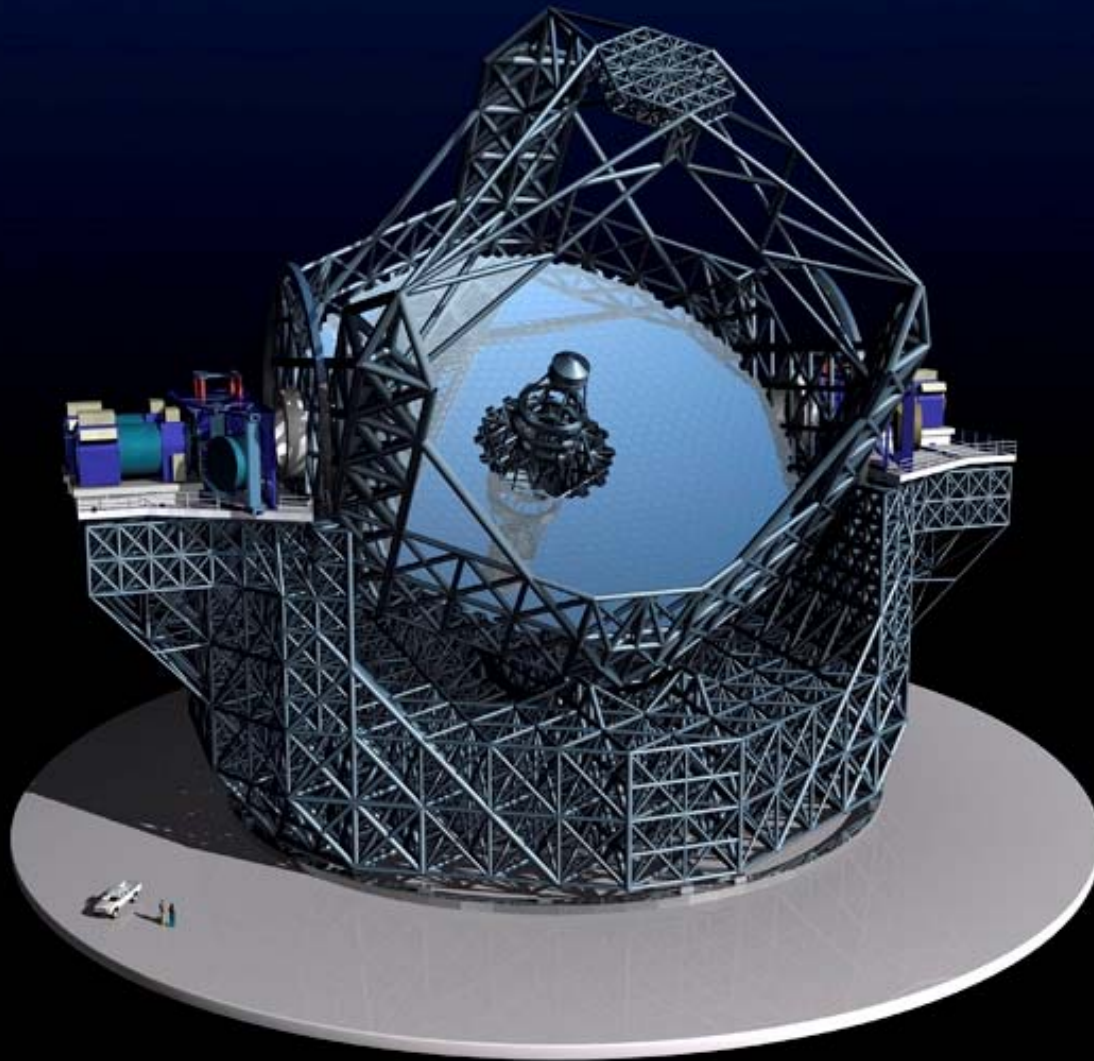
The answer is 42, but what was the question?  
(from *The Hitchhiker's Guide to the Galaxy*)

We discuss the potential of the 42m E-ELT at 2 - 5 microns (broad band and narrow band filters) to probe the number density and brightness of deeply embedded massive stars and young stellar objects just formed in dense Galactic proto-cluster molecular clouds (ultracompact HII regions, hot cores, outflow and maser sources), penetrating as much as 200 mag of visual extinction. The combination of precise astrometric, proper motion (1mas/yr) data and high-spectral resolution, radial velocity ( $R \geq 10^4$ ) data are crucial to study dynamical processes associated with cluster formation, such as tight massive binary formation and gravitational interactions followed by slingshot stellar ejections (runaway stars). Integral field spectroscopy is needed of these dense and crowded clusters (up to 100 objects per square arcsec at apparent magnitudes  $K = 25-28$ ).

# talk outline

1. The 42m E-ELT
  - science cases
  - instruments
  - resolution
  - sensitivity
2. Interstellar extinction in the Infrared
3. DRM proposal: The origin of massive stars  
(a particular science case for the E-ELT)
  - embedded dense stellar population
  - embedded stellar (and gas) dynamics
4. Some examples of dense young star clusters
5. summary and conclusions (synergy with ALMA)

E-ELT



[http://www.eso.org/sci/facilities/eelt/science/drm/tech\\_data/instruments](http://www.eso.org/sci/facilities/eelt/science/drm/tech_data/instruments)

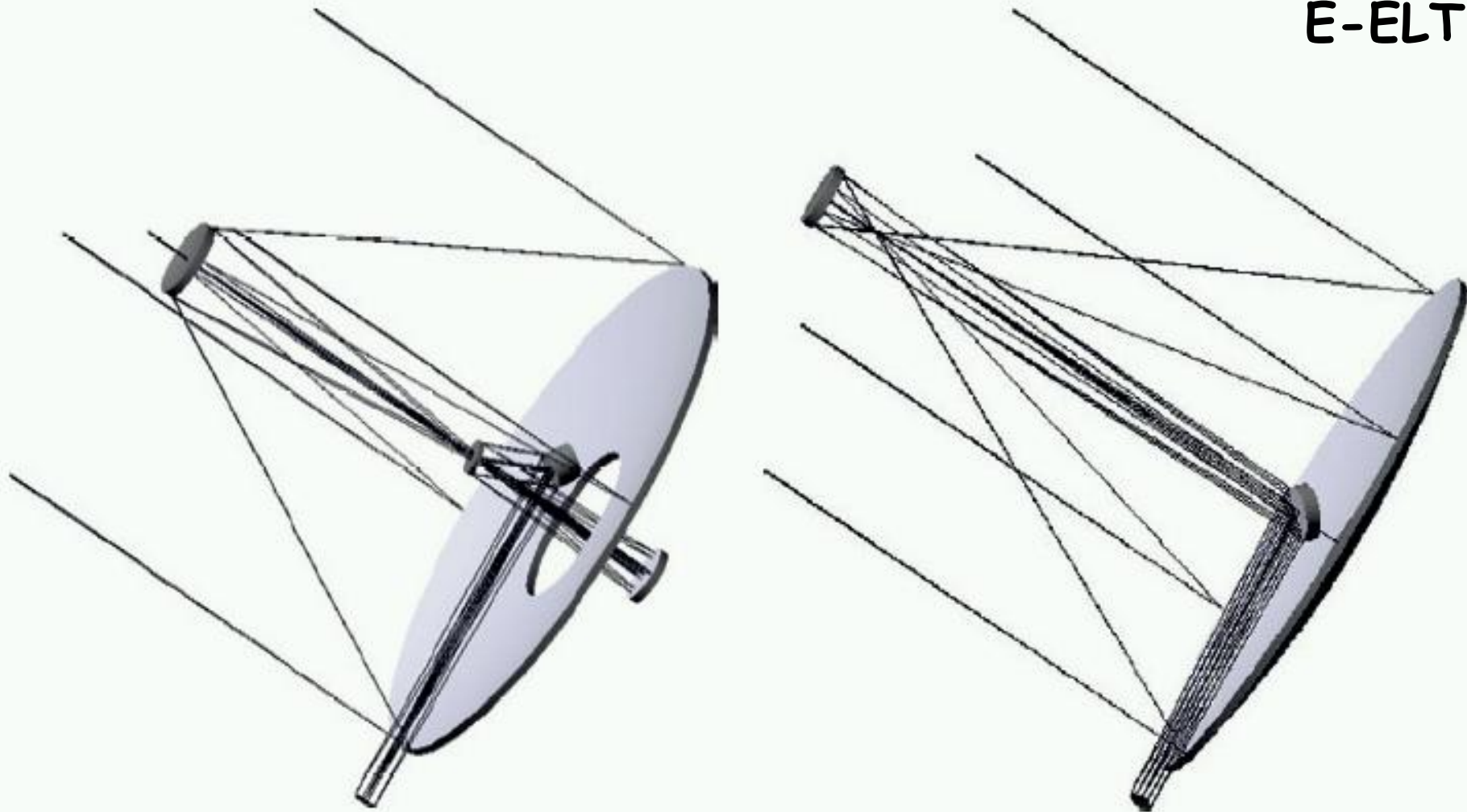


Figure 1: The two optical designs considered during the Basic Reference Design development: five-mirror (left) and Gregorian (right).

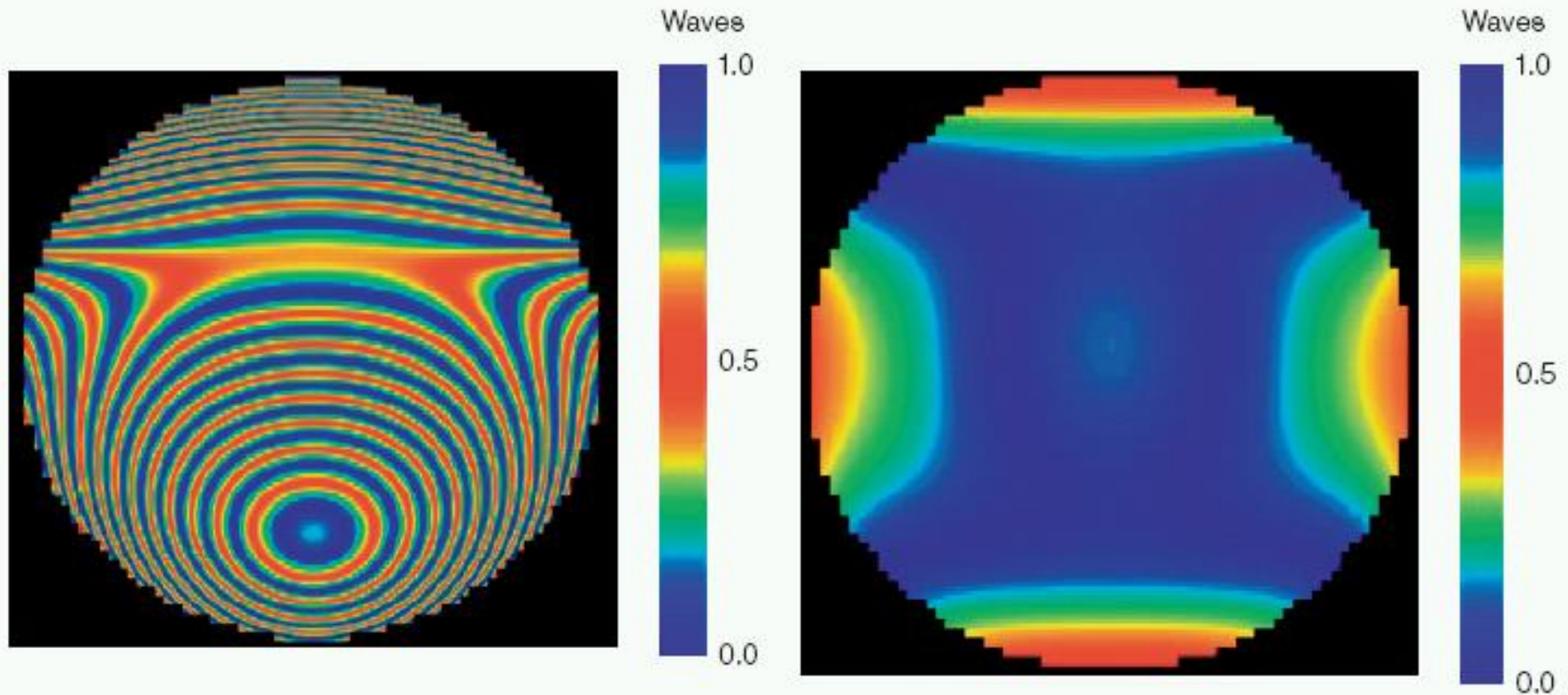


Figure 5: Wavefront aberrations in the laser guide stars. The five-mirror design (right) has a clear advantage over the Gregorian (left).



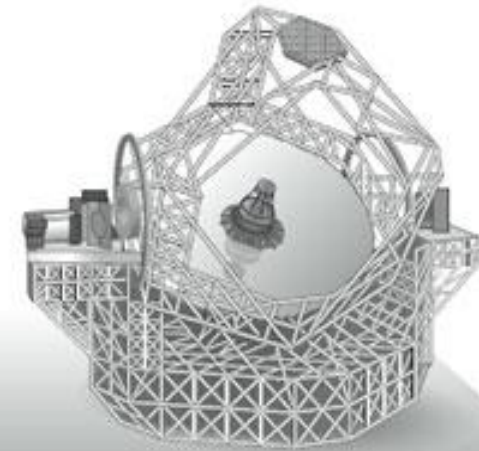
Big Ben clocktower  
(96.6 metres) for scale



Giant Magellan Telescope



Thirty-Meter Telescope



European Extremely Large Telescope

<b>Telescope diameter</b>	25.2 metres	30 metres	42 metres
<b>Component mirror segments</b>	7 (8.4-metre segments)	492 (1.44-metre segments)	984 (1.45-metre segments)
<b>Cost</b>	US\$600 million	US\$754 million	€900 million (US\$1.37 billion)
<b>Planned location</b>	Chile	Candidates: Hawaii; Mexico; three sites in Chile	Candidates: Canary Islands; Morocco; Argentina; two sites in Chile
<b>Planned construction period</b>	2010–2017 (First mirror already cast)	2009–2016	2010–2017
<b>Technical advantages</b>	Adaptive optics integrated within secondary mirror Shortest focal length means it has the smallest and cheapest structure	Mirror segments are comparatively cheap and more easily replaced Similar scaled-up version of the existing Keck telescopes	Five-mirror design results in a flat focal plane and better images Similar mirror-segment size to the TMT, so greater vendor choice
<b>Financial advantages</b>	Potential support from \$34-billion Harvard endowment or Texas billionaire George Mitchell	\$200-million gift from Intel founder Gordon Moore	Steady European funding stream
<b>Disadvantages</b>	Only one place can make the mirrors Gaps in mirror limit the effective aperture to 21.5 metres	Adaptive optics performed after the light leaves the telescope, so the 'natural seeing' mode cannot benefit from adaptive corrections to wind effects	Biggest and most expensive design No similar design experience Reflections through five mirrors reduce light levels

Cumulative area (square metres)



# THE E-ELT DESIGN REFERENCE MISSION

---

## DRM SCIENCE CASES

The following is the list of 'prominent' science cases chosen by the SWG to be studied by the DRM:

- Planets & Stars
  - S3: From giant to terrestrial exoplanets: detection, characterization and evolution (demo case)
  - S9: Circumstellar disks
  - S5: Young stellar clusters and the Initial Mass Function
- Stars & Galaxies
  - G4: Imaging and spectroscopy of resolved stellar populations in galaxies (demo case)
  - G9: Black holes and AGN
- Galaxies & Cosmology
  - C10: The physics of high redshift galaxies (demo case)
  - C4: First light - the highest redshift galaxies
  - C7: Is the low-density intergalactic medium metal enriched?
  - C2: A dynamical measurement of the expansion history of the Universe

The letter/number combinations refer to the science case designations in the SWG's first report.

## INSTRUMENTS

The following table lists the instruments that are 'available' for DRM simulations. Please note that this is a list of 'virtual' instruments intended to serve as a starting point for the DRM only. This should *not* be taken to reflect any priorities or to represent a list of real instruments to be studied for the E-ELT.

Instrument	Wavelength range [μm]	AO mode	Field of view and sampling	Comments
Diffraction Limited Imager (DLI)	0.7–2.5	LTAO or MCAO	30"×30" 2.5 mas/pix	Desired: up to 2'×2' FoV with 10 mas/pix. Lower λ limit set by detector.
Single field IFU	0.5–2.5 split between two arms	LTAO or MCAO	1"×1" 5 mas/pix or 10"×10" 50 mas/pix	Lower λ limit set by trade-off between resolution, spectral coverage in one shot and efficiency. R=3000–20000. R=3000 covers at least one band (J,H,K). Coverage in one shot to be studied for R=20000.
Multi-field IFU	0.7–2.5	MOAO, possibly GLAO or MCAO	Circular patrol field: 5' diameter Individual IFUs: ~1.3"×1.3" 50–75 mas/pix	Lower λ limit set by detector. R=3000 (covering at least one band in one shot). Multiplex ≥ 20. Desirability of a larger patrol field up to D=8' to be justified.
XAO imager and IFU	0.6–1.8 (goal: 2.4)	XAO, 200×200 actuators	2.5"×2.5" Nyquist sampling of diffraction limited core at 600 nm (TBD)	R=50 (Y–H). Polarimetry + classical imaging (600–900 nm). High resolution spectroscopy TBD.
Ultra-stable high resolution spectrograph (HRS)	0.38–0.7	Seeing limited	1"×1"	R=150000. Full spectral coverage in 1 shot. Multiplex=1.
Mid-IR imager	L–Q	LTAO?	35"×35" 3–5 μm: 9 mas/pix 5–25 μm: 17 mas/pix	Narrow and broad band filters.
and IFU	3–25	LTAO?	1"×1" sampling at 1.5×FWHM	R=500, one band in one shot. R=3000, spectral coverage in one shot = $\lambda_c/3$ . R=50000, spectral coverage in one shot = $\lambda_c/50$ .

## Diffraction limit ( $\sim \lambda/D$ ) of a $D=42\text{m}$ telescope:

at 2 micron	$\sim 10\text{mas}$
at 3 micron	$\sim 15\text{mas}$
at 5 micron	$\sim 25\text{mas}$

astrometric precision at 2 microns:  $1\text{ mas/yr}$  ( $20\text{ km/s}$  at  $4\text{ kpc}$ )

# sensitivity limit ( $\sim D^4$ ) of a $D=42\text{m}$ telescope

(for point sources, background-noise limited)

$K = 28 \text{ mag}$  (see ELT exposure time calculator)

$L = 22 \text{ mag}$  (about 7 mag deeper than 8m VLT)

$M \sim 20 \text{ mag}$  (Paranal sky background  $1.2 \text{ mag}/\square''$ )

for  $S/N = 10$  in  $t = 1$  hour integration time

(for a given  $S/N$ ,  $t_{\text{integration}} \sim D^{-4}$ )

PS.

compare these numbers with MATISSE performance...

VLT 2<sup>nd</sup> gen 4-element interferometer, 3-10 micron

$L = 8.5 \text{ mag}$  for  $S/N = 5$  in 1 hour integration time

# Interstellar Extinction in the Infrared

(Rieke and Lebofski 1985, D. Lutz 1999)

$$A_J = 0.28 A_V \quad A_L = 0.06 A_V$$

$$A_H = 0.18 A_V \quad A_M = 0.02 A_V$$

$$A_K = 0.11 A_V$$

for  $A_V = 200$  mag ( $N_{H_2} = 10^{23.5}$  cm<sup>-2</sup>)

ie. a dense protocluster cloud clump

$$A_J = 56 \text{ mag} \quad A_L = 12 \text{ mag}$$

$$A_H = 36 \text{ mag} \quad A_M = 4 \text{ mag}$$

$$A_K = 22 \text{ mag}$$

**HERE IS THE KEY MESSAGE TO TAKE HOME:**

a 42m ELT can penetrate  $A_K = 22$  mag

of extinction in the K-band to detect

deeply embedded luminous massive stars ( $A_V = 200$  mag)

in addition, there are the hydrogen recomb.

lines  $Br_g$ ,  $Pf_g$ ,  $Br_a$ ,  $Hu$  (14-6)

whose ratios have well-defined values

(e.g.  $Br_g/Br_a = 1/3$ ;  $Br_g/H_\alpha = 1/100$ )

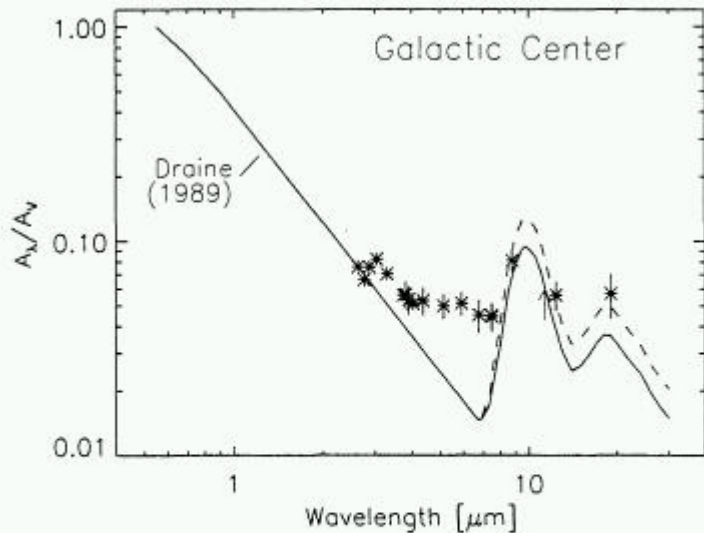
in optically thin ionised gas (Menzel Case B)

to infer the extinction to individual objects

# ISO OBSERVATIONS OF THE GALACTIC CENTRE

D. Lutz

Max-Planck-Institut für extraterrestrische Physik, Garching, Germany



Because of its well-known and fairly homogeneous foreground extinction, the Galactic Centre is uniquely suited for studies of the mid-infrared extinction law. Our results indicate significantly higher extinction in the 3-8  $\mu\text{m}$  region than usually assumed.

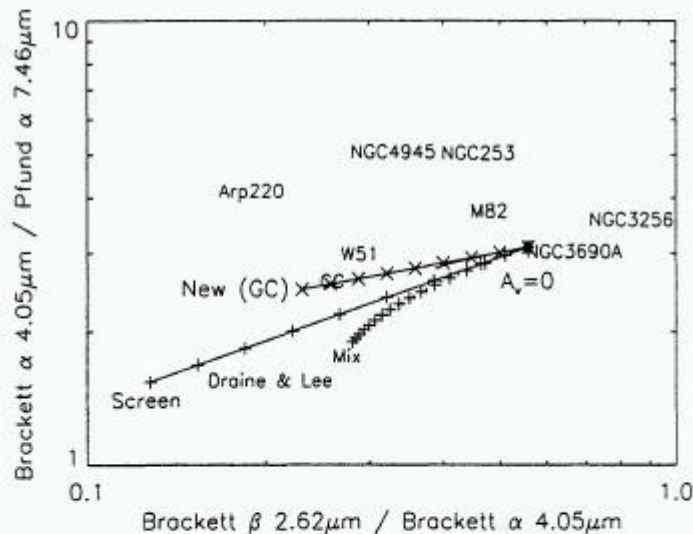
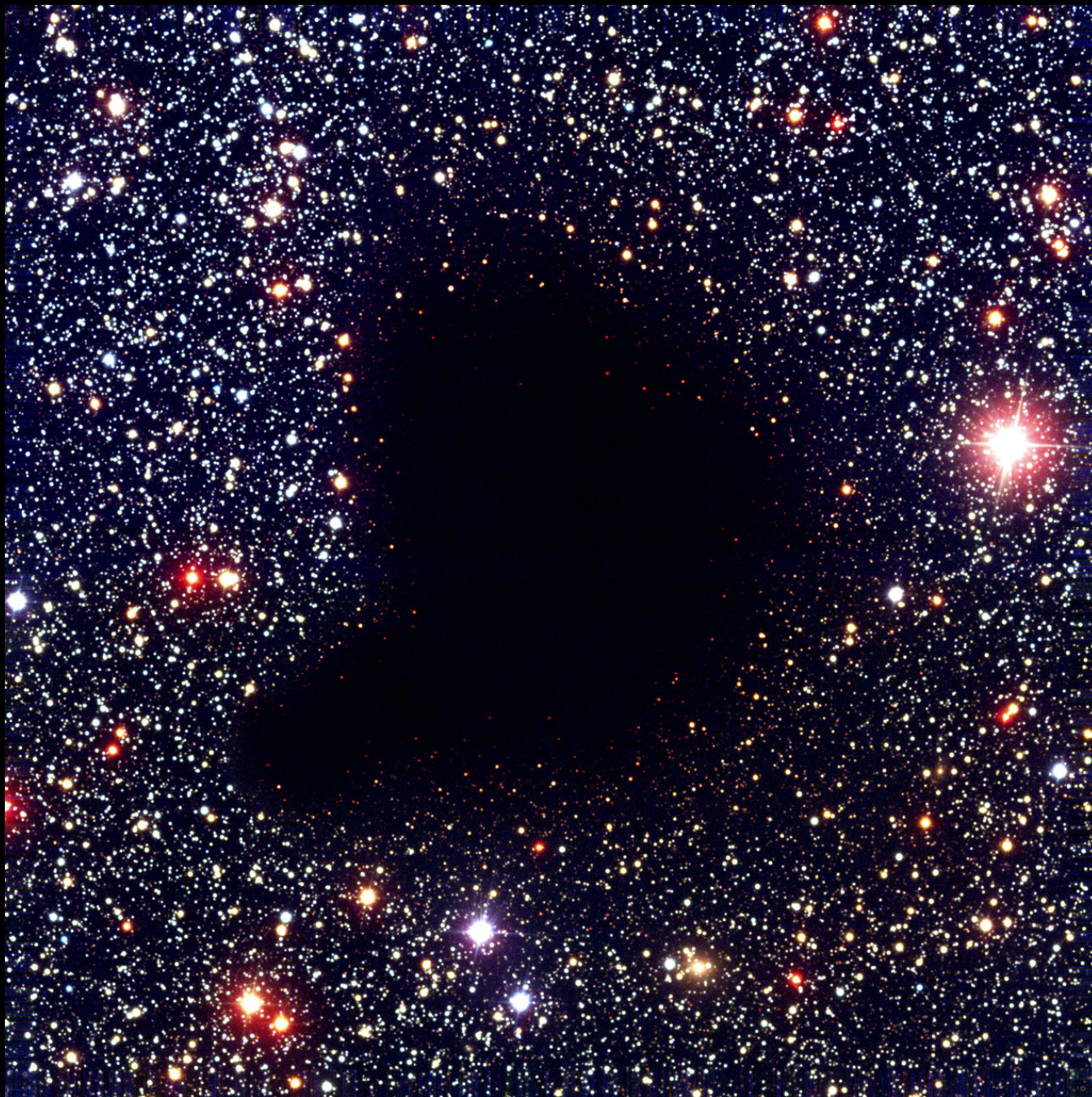


Figure 5. Top: Mid-infrared extinction law derived from hydrogen recombination line observations of the Galactic center, compared to the one given by Draine (1989). Bottom: Observed recombination line ratios in several galaxies and star forming regions compared to expectations for a standard extinction law

The Universe as Seen by ISO.  
Eds. P. Cox & M. F. Kessler.  
1999. ESA-SP 427. p. 623

B 68 dark cloud

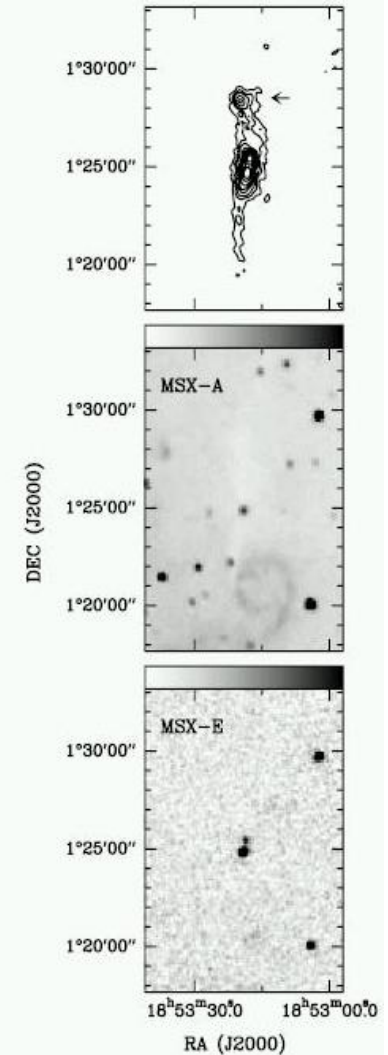
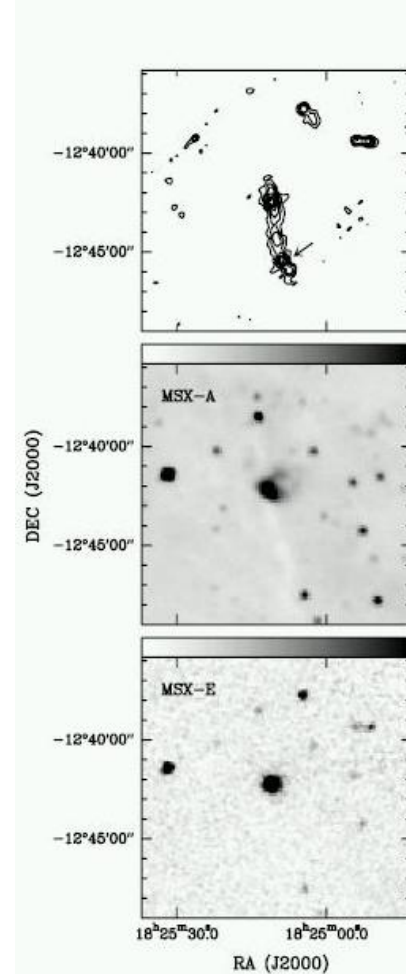
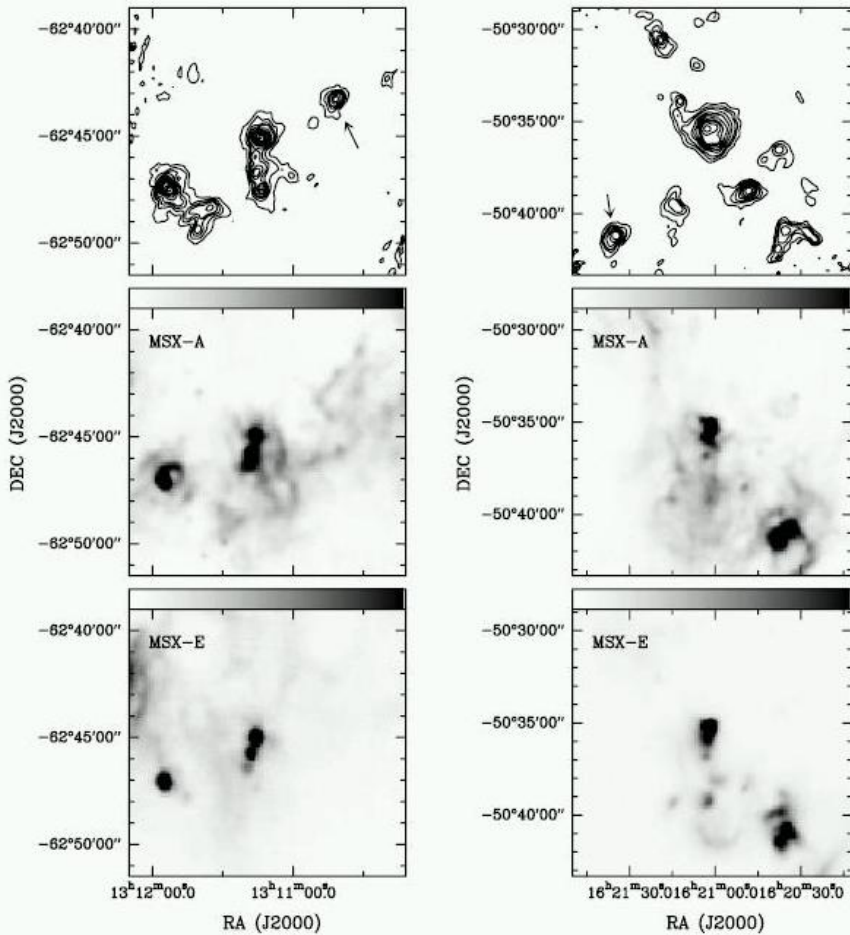


credit: J. Alves, ESO



Looking Through the Dark Cloud B68 (NTT + SOFI)

Typical gas densities  $2 \cdot 10^5 \text{ cm}^{-3}$ , sizes  $\sim 0.5 \text{ pc}$   
 $\Rightarrow N_{\text{H}_2} = 3 \cdot 10^{23} \text{ cm}^{-2} \quad \Rightarrow A_V = 200 \text{ mag}$



1.3mm dust continuum observations (contours, top row)  
of 4 dense molecular proto-cluster regions

MSX mid infrared images of the same regions

**DRM proposal: The origin of massive stars  
(a particular science case for the E-ELT)**

- embedded dense stellar population**
- embedded stellar (and gas) dynamics**

**the centers of young massive clusters**

# ELT near-infrared and thermal-infrared studies of massive star formation: direct imaging and integral field spectroscopy of ultracompact HII regions

Hans Zinnecker

Astrophysikalisches Institut Potsdam, An der Sternwarte 16, 14482 Potsdam, Germany  
email: hzinnecker@aip.de

**Abstract.** In this contribution, we show how a future ELT (>25 m diameter) helps to understand the formation and early dynamical evolution of massive stars embedded in dust-enshrouded very compact HII regions. We describe how to exploit the ELT's near- and mid-IR enhanced sensitivity and high angular resolution to peer through huge amounts of dust extinction, taking direct nearly diffraction-limited images and doing IFU spectroscopy. Together with ALMA, an ELT will be a powerful observing platform to reveal one of the most hidden secrets of stellar astrophysics: the origin of massive stars.

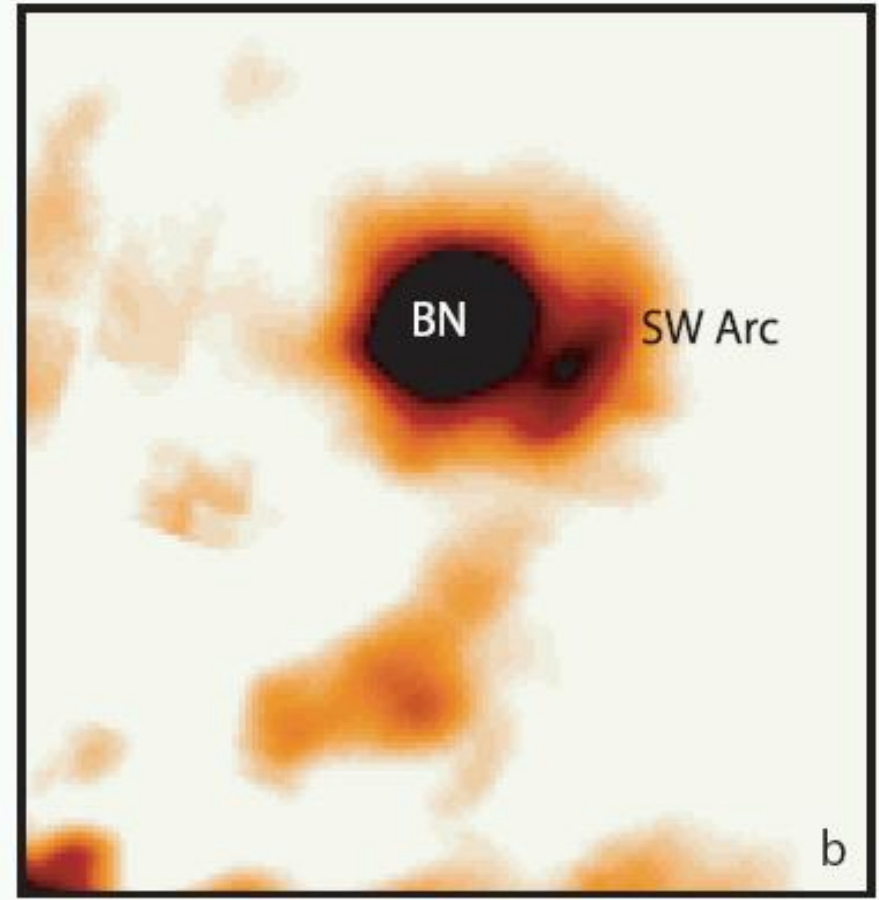
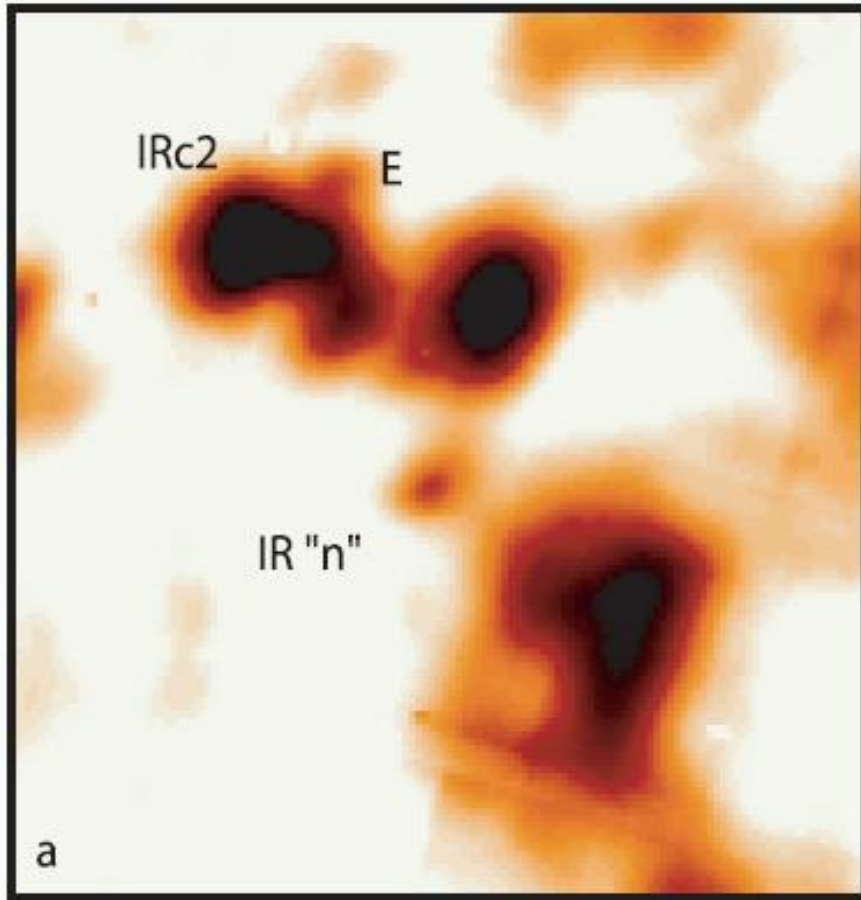
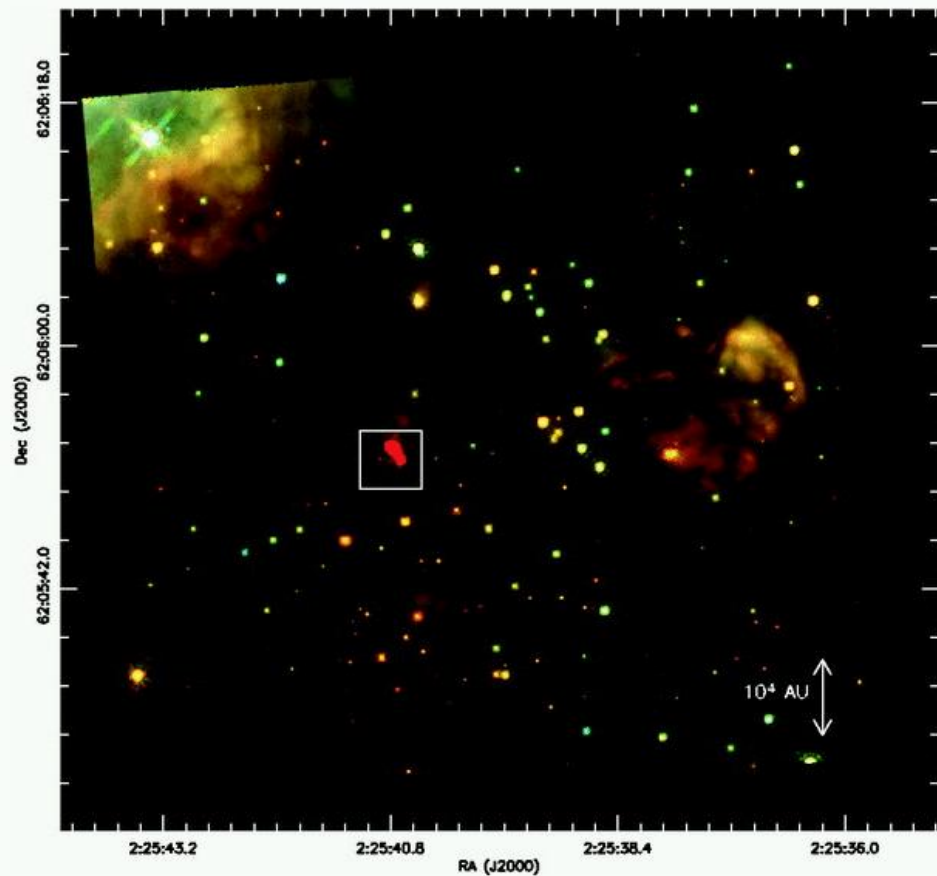


FIG. 3.—Detailed  $12.5 \mu\text{m}$  sub-images ( $10'' \times 10''$ ) enhancing low-level emission around (a) near-IR source n and (b) the BN SW arc.

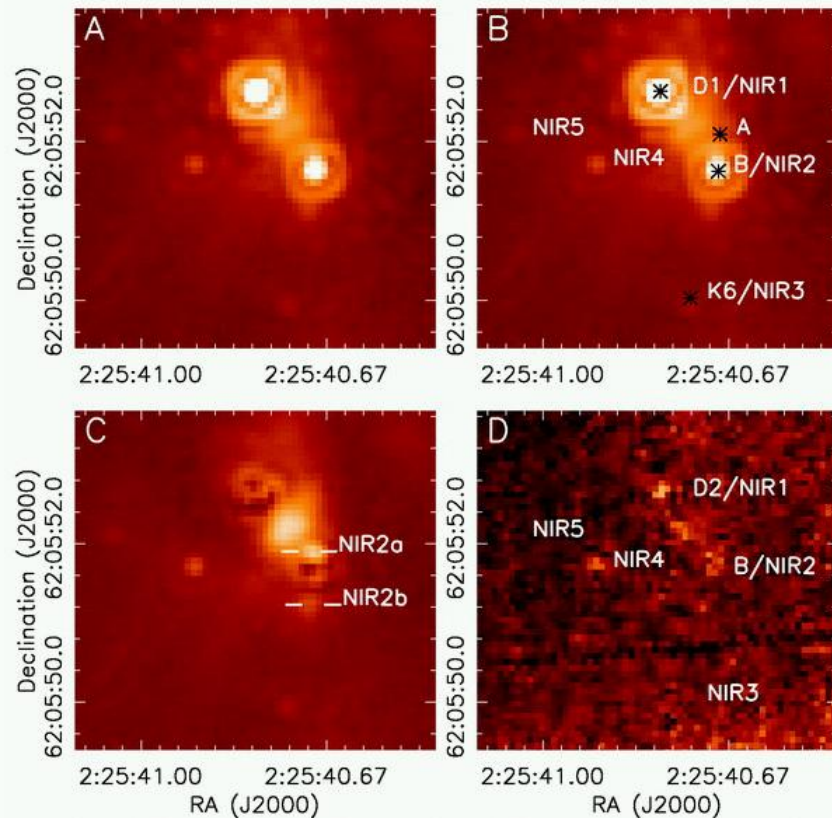
mid infrared images of the  
Orion KL-BN region

**Fig. 2**  
Color-composite image constructed from the F110W (*blue*), F160W (*green*), and F222M (*red*) mosaics of the W3 IRS 5 region, encompassing the whole region surveyed in the NICMOS measurements. The box shows the region displayed in Fig. 3.



W3 IRS 5 with NICMOS

**Fig. 3**  
F222M (2.22  $\mu$ m) and F160W (1.60  $\mu$ m) images of W3 IRS 5 and the neighboring red sources and nebulosities. In panel A we show the F222M image using a cube root scaling. In panel B we show the same image, but with the main NIR sources marked. The asterisks mark the positions of the associated radio sources D2, B, A, and K6. In panel C we show the image with the NIR 1 and NIR 2 sources subtracted. An extended nebulosity between the two sources is clearly evident. Two additional point sources partially hidden by the PSF of NIR 2 are marked. The ringlike pattern is a residual from the PSF subtraction. In panel D we show the F160W image toward this region, with the five IR sources marked.



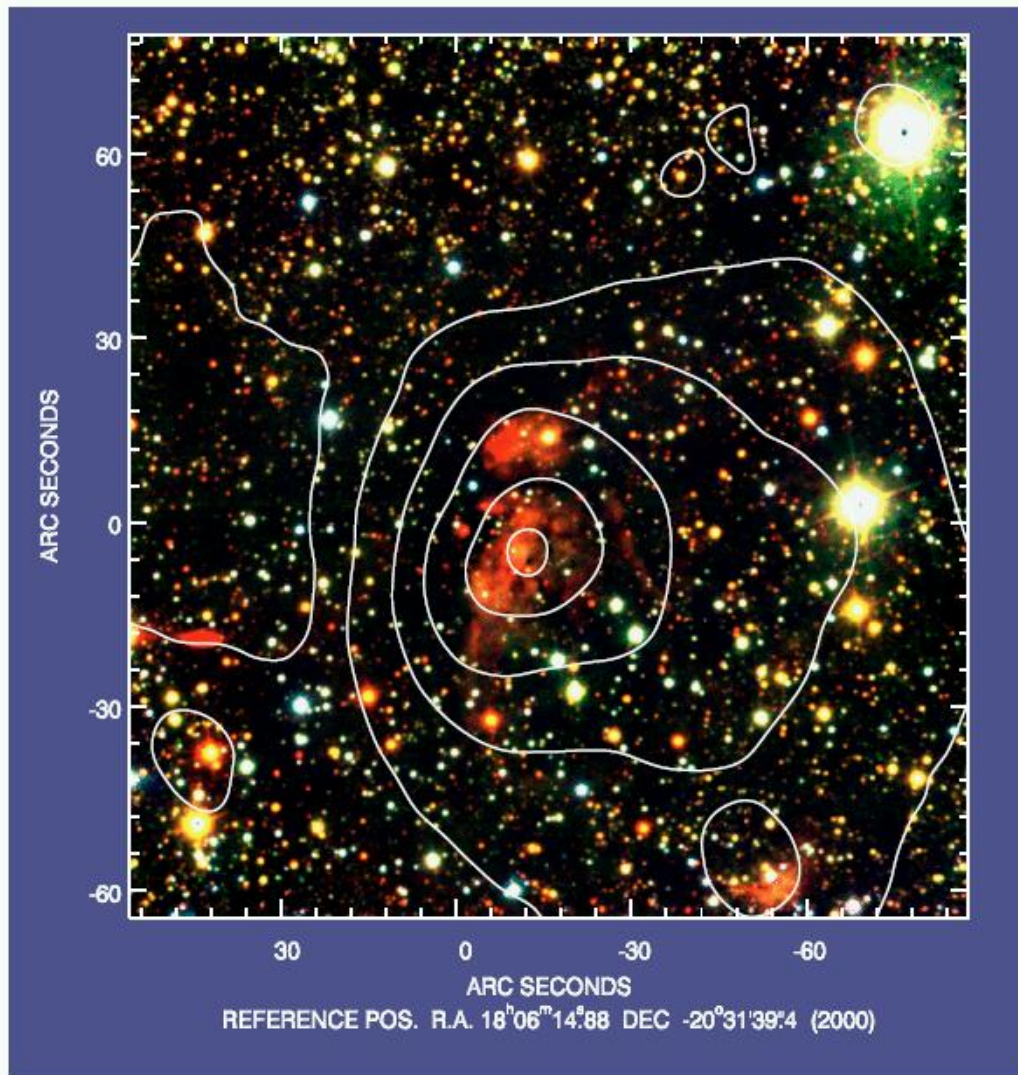


**Fig. 1.** Colour-coded image of the entire G9.62+0.19 region taken in the three broad-band NIR filters  $J$  (blue),  $H$  (green), and  $K_s$  (red). The large-scale contour lines denote the emission levels derived from the  $8.28 \mu\text{m}$  image of the related  $MSX$  source. The left-most large contour line indicates the position of the close-by Infrared Dark Cloud.

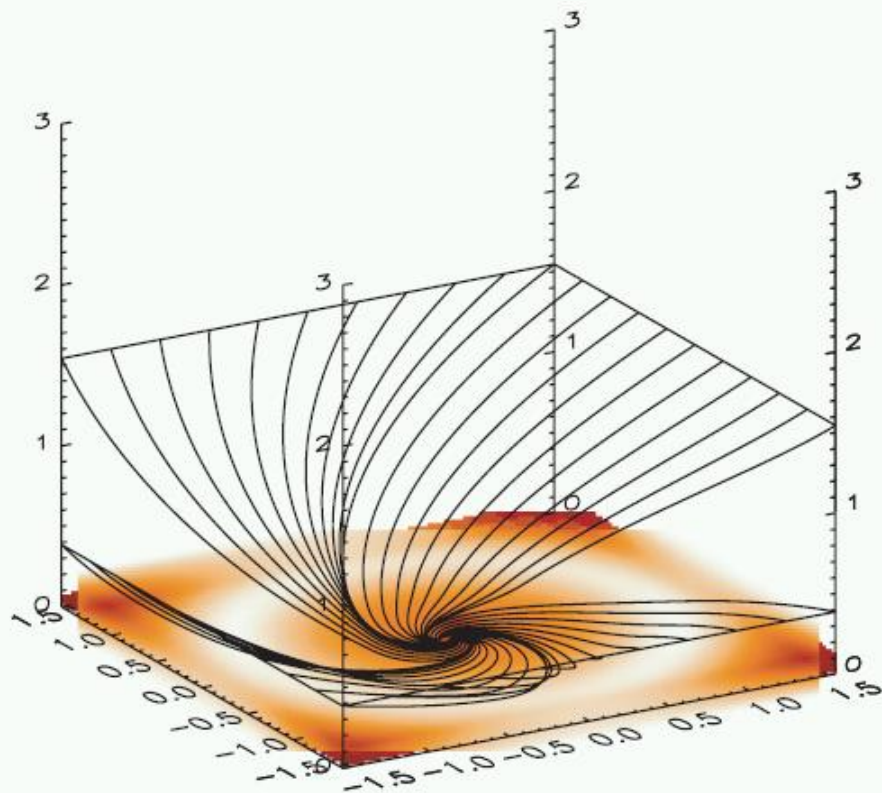


FIG. 9.—Streamlines of a model of an accretion flow with the gas in ballistic trajectories around a point mass. The gas starts in a quasi-spherical infall, and owing to conservation of angular momentum, spins up until a rotationally dominated disk forms at a nondimensional radius of unity. The model demonstrates the structure of the accretion flow onto the cluster G10.6–0.4 that shows quasi-spherical infall on the larger scales in the molecular gas, and disk accretion on the smaller scales in the ionized gas.

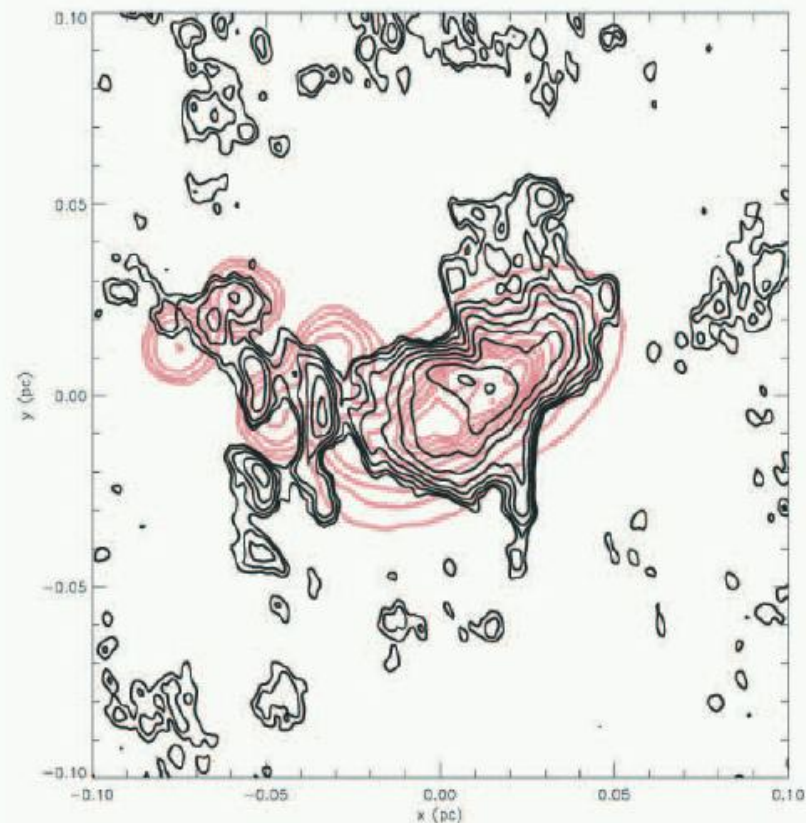


FIG. 10.—Model of the continuum emission at 1.3 cm from star cluster G10.6–0.4, on top of the observed radio continuum. The model shows an ionized accretion disk and ionized globules in the clumpy gas around the disk. The model is a Terebey et al. (1984) accretion disk with a centrifugal radius of 3500 AU, and an infall rate of  $10^{-4} M_{\odot} \text{ yr}^{-1}$  onto a  $500 M_{\odot}$  cluster with additional density fluctuations imposed on the otherwise smooth structure of the underlying accretion flow. The angular scale is set for a distance of 6 kpc. The contour levels in the data start at  $1 \text{ mJy beam}^{-1}$  and increase in half magnitude levels.

stellar and gas dynamics in dense embedded proto clusters

remember  $1 \text{ mas/yr} = 20 \text{ km/s}$  at 4 kpc

also note  $R = 10^4$  spectral resolution = 30 km/s

the combination of astrometry and radial velocity  $\Rightarrow$  star/gas dynamics

Cluster/ID	Multiplicity	Sp. Types	P (days)	M2/M1
<b>NGC 6231</b>				
CPD-41°7742	ESB2	O9V+O9.5V	2.44	0.56
HD 152219	ESB2	O9III+B1-2V/III	4.24	0.39
HD 152248	ESB2	O7III(f)+O7.5III(f)	4.82	0.99
HD 152218	SB2	O9IV+O9.7V	5.6	0.76
CPD-41°7733	SB2	O8.5V+B3	5.68	0.38
WR 79	SB2	WC7+O6V	8.89	0.37
HD 152234	SB2	O9.7I + O8V	126.6	0.83
HD 152247	SB2	O9III+O9.7V	~500	0.64
HD 152233	SB2	O6III(f)+ O8V:	~800	0.6
HD 152314	SB2	O8.5V+B1-3V	~3100	0.53
HD152076	single	O9.5III		
HD152200	single ?	O9.7V		
HD 152249	single	O9Ib((f))		
HD326329	single	O9.5V		
HD326331	single	O8III((f))		
CPD-41 7721	single	O9V		
<b>IC 2944</b>				
HD 101205	ESB2	O7V+OB:	~2	0.55
HD 101190	SB1	O6.5V	~8	
HD101131	SB2	O6V+O8.5V	9.6	0.61
HD100099	SB2	O9V+O9.5V	~20d	0.91
HD 101436	SB2	O7.5V+B0V	>20d	0.52
HD101413	SB2	O9III+B	Long P	0.45
HD 101191	SB1	O8V	Long P	
HD101298	single	O8V		
HD 101223	single	O7.5V		
CPD-62 2198	single	O9.5III		
HD101333	single	O9.5V		

Hughes Sana (priv. commun.)

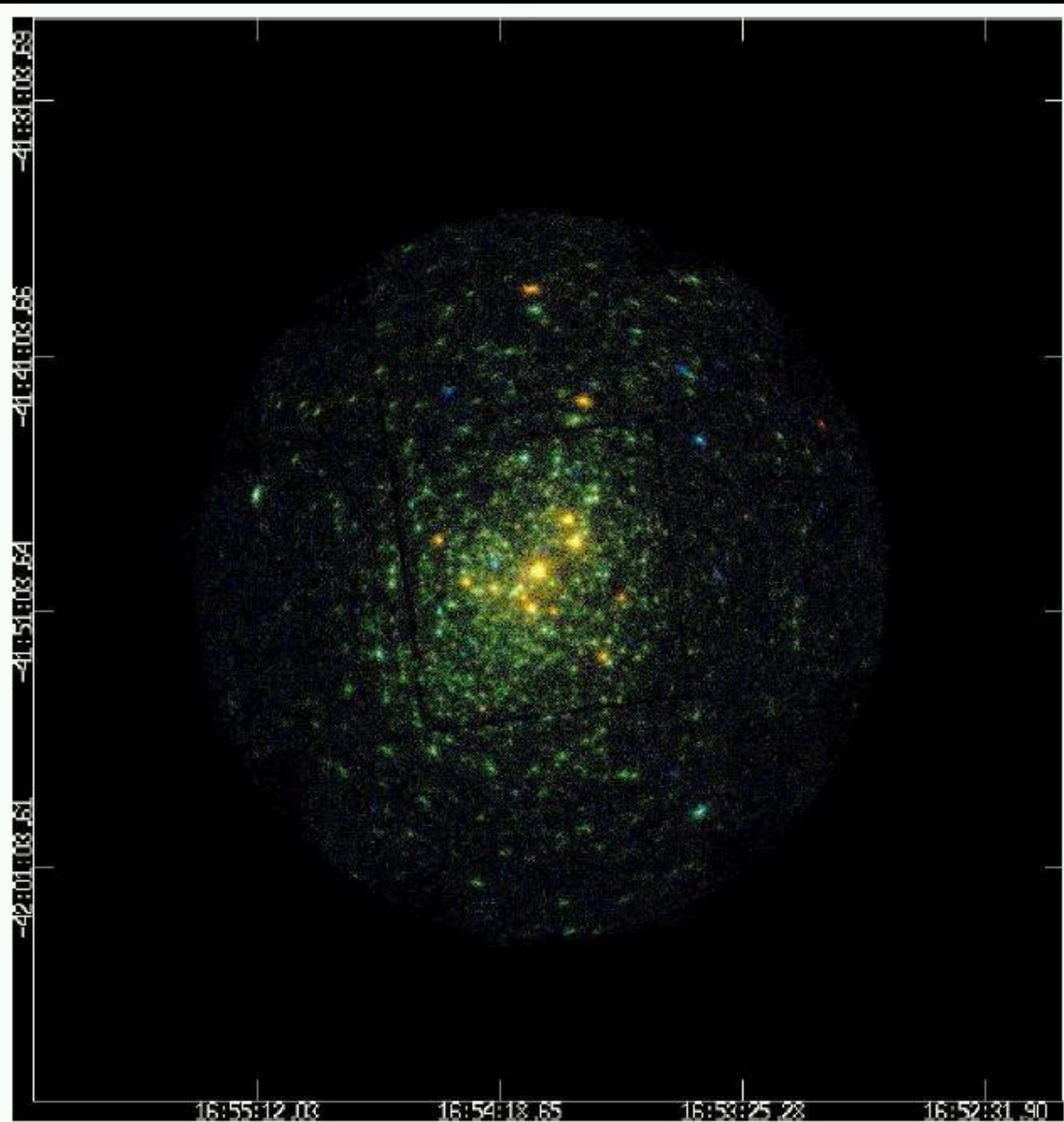


Fig. 1. Combined EPIC MOS three-color X-ray image of the young open cluster NGC 6231. The field is roughly 30' in diameter and is centered on HD 152248. North is up and East is to the left. The different colors correspond to different energy ranges: red: 0.5-1.0 keV; green : 1.0-2.5 keV; blue : 2.5-10.0 keV.

Sana et al. 2008

## INTEGRAL FIELD SPECTROSCOPY

Definition „spaxel“

4k x 4k IR detectors (K, LM)

pixel scale: 5 mas (K), 10 mas (LM)  $R = 10^4$

IR stellar spectroscopy in crowded cluster centers

e.g.  $Br_g$  (2.17  $\mu$ ),  $Br_a$  (4.05  $\mu$ ); CO 2.3  $\mu$ , 4.6  $\mu$

**ELT**

# The ~~VLT~~ and powers of 10: young clusters home and away

Hans Zinnecker

Astrophysikalisches Institut, Potsdam, Germany

**Abstract.** The purpose of this short paper is to remind the European star formation community, and more specifically the European young star clusters community, of the great potential of the VLT and to encourage the young European astronomers to make more and better use of it. Three classical examples of very young star clusters at 500 pc, 6.5 kpc, and 55 kpc (the Orion Nebula Cluster, NGC 3603 in the Carina arm, and R136 in the LMC) are chosen to illustrate the resolving power of the VLT in direct imaging mode, adaptive optics mode, and interferometric mode. The VLT with its high spatial resolution modes can be used as an astronomical microscope, as it were, with a zoom factor of 10 to 100.

**Table 2.** Major southern clusters (home and away)

VLT targets	distance	m - M
Rho Oph	125 pc	5.5
Orion TC	500 pc	8.5
NGC 3603	6.5 kpc	14.0
R136	55 kpc	18.5
NGC 5253	4 Mpc	28.0
Antennae	20 Mpc	31.5

Orion Nebula and Trapezium Cluster (J,K,L true-colour composite)



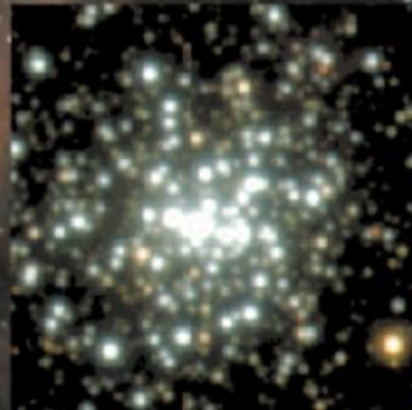
Orion

Credit:  
McCaughrean & Rayner

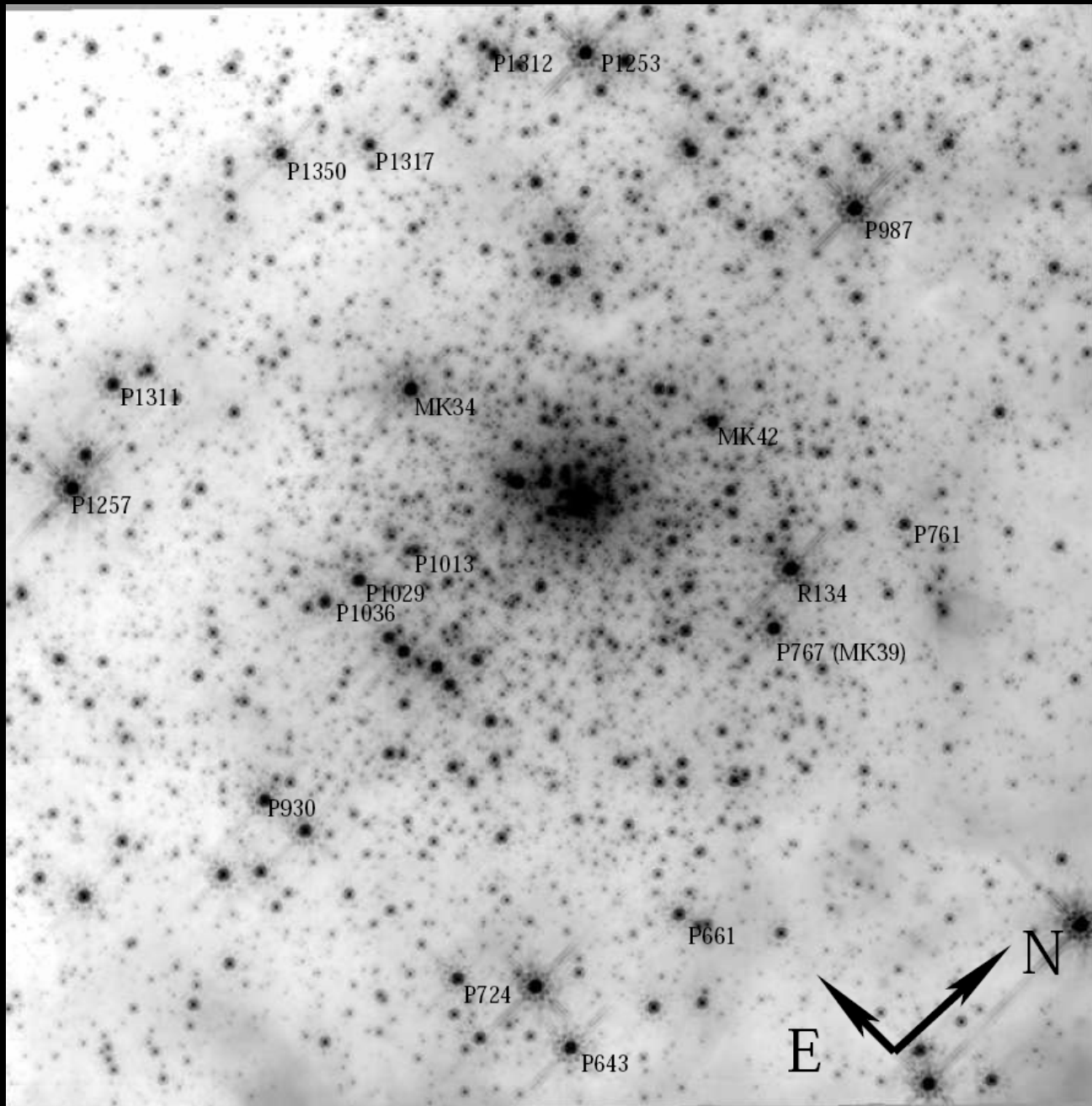
NGC 3603

VLT/ISAAC JHK

FOV 3.4' x 3.4'



Brandl et al. 1999



R 136 (NGC 2070)

HST/NICMOS image

FOV 15 pc x 15 pc

Andersen et al. 2007



R136 cluster

HST  
optical/IR image

FOV  $\sim 30'' \times 30''$

Zinnecker 2004

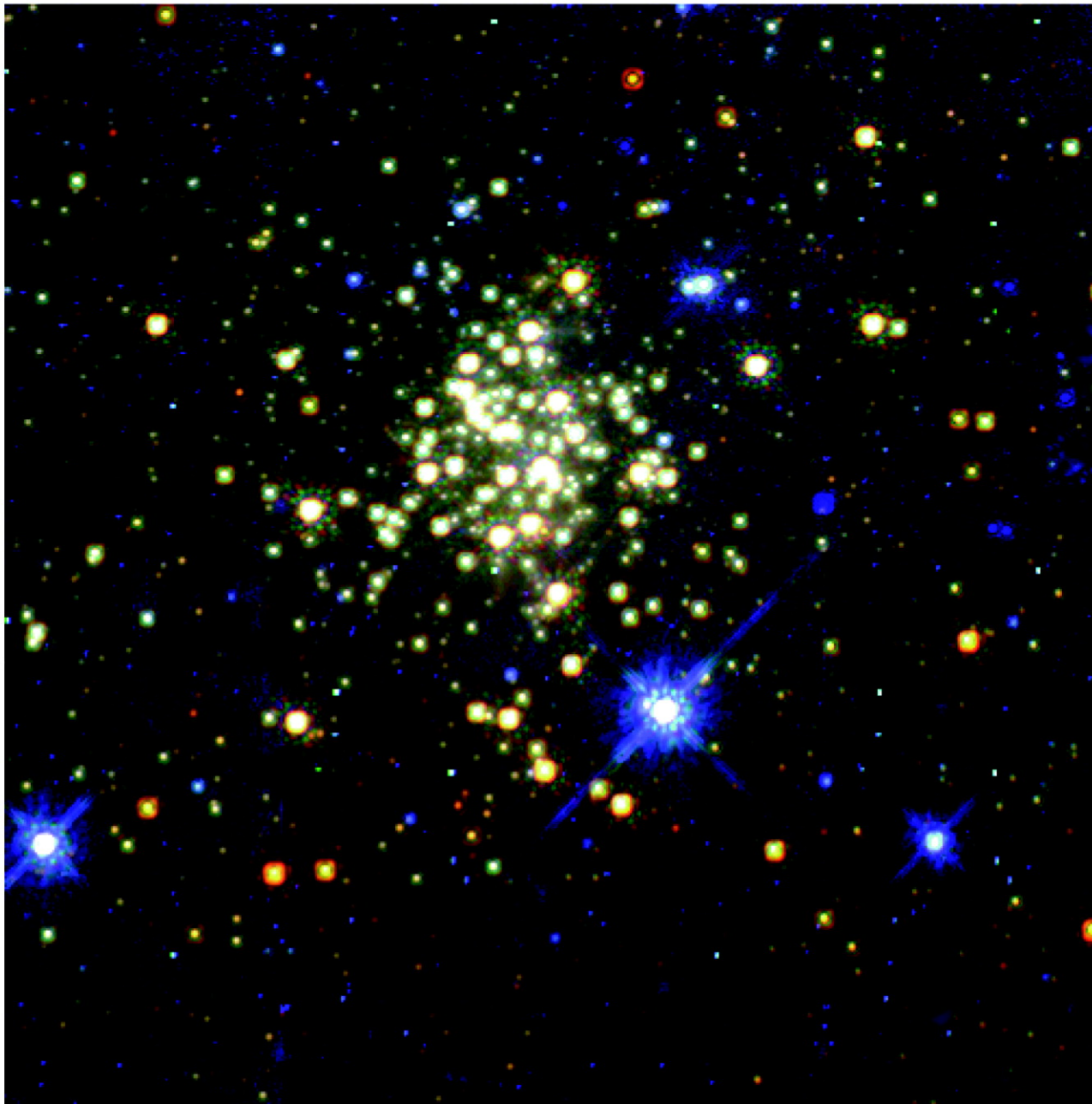


Westerlund 1 cluster

NTT/SOFI JHK image

FOV  $\sim 4 \times 4$  arcmin

Brandner et al. 2007



Arches cluster

Color composite image  
F205W (*red*),  
F160W (*green*),  
and F110W (*blue*)

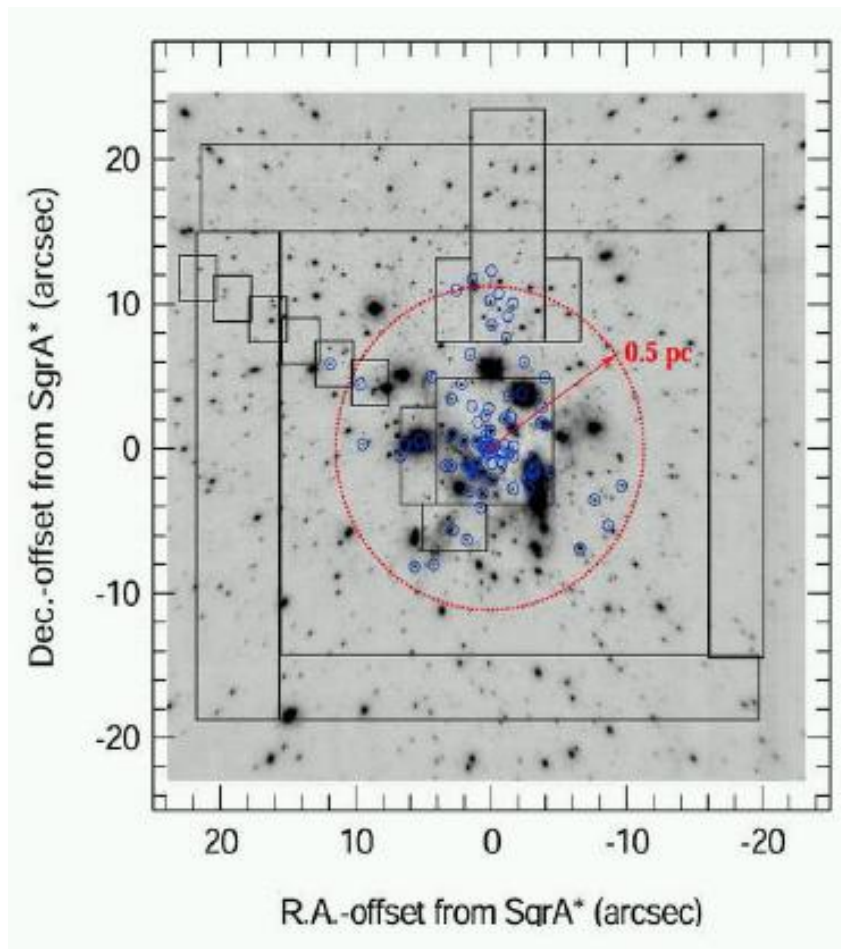
Figer et al. 1999



Quintuplet cluster

Color composite image  
F205W (*red*),  
F160W (*green*),  
and F110W (*blue*)

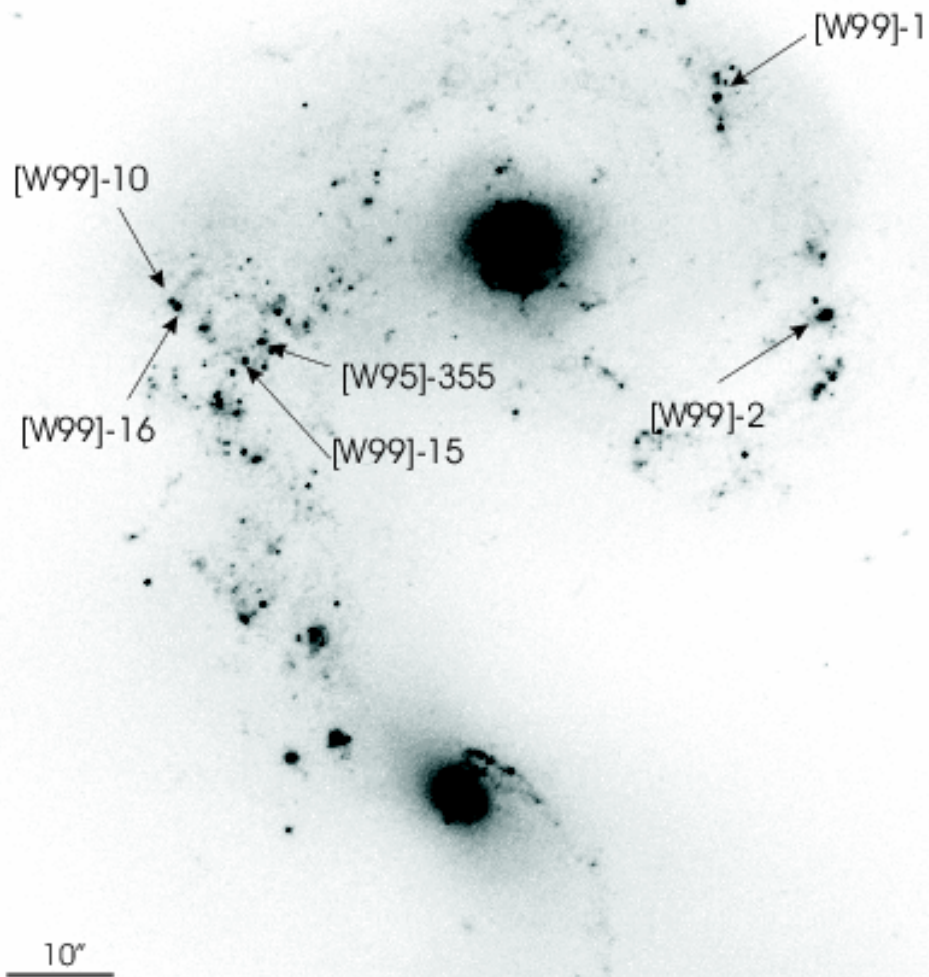
Figer et al. 1999



Outline of the various 2003-2005 SPIFFI/SINFONI H+K- and K-band cubes, superposed on a  $\sim 100$  mas resolution, L-band NACO image (logarithmic scale). Small circles denote the 90 quality 1 and 2 early-type stars (OB I-V, Ofpe/WN9, W-R stars. A dotted circle denotes a 0.5 pc (20 arcsec) radius zone centered on Sgr A\*, within which essentially all OB stars we have found appear to lie (from Paumard et al. 2006).

NGC 4038/4039

ISAAC Ks-band image



## CLOUDSHINE: NEW LIGHT ON DARK CLOUDS

JONATHAN B. FOSTER AND ALYSSA A. GOODMAN

Harvard-Smithsonian Center for Astrophysics, 60 Garden Street, Cambridge, MA 02138

*Received 2005 October 22; accepted 2005 November 10; published 2005 December 16*

### ABSTRACT

We present new deep near-infrared images of dark clouds in the Perseus molecular complex. These images show beautiful extended emission that we model as scattered ambient starlight and name “cloudshine.” The brightness and color variation of cloudshine complicates the production of extinction maps, the best tracer of column density in clouds. However, since the profile of reflected light is essentially a function of mass distribution, cloudshine provides a new way to study the structure of dark clouds. Previous work has used optical scattered light to study the density profile of tenuous clouds; extending this technique into the infrared provides a high-resolution view into the interiors of very dense clouds, bypassing the complexities of using thermal dust emission, which is biased by grain temperature, or molecular tracers, which have complicated depletion patterns. As new wide-field infrared cameras are used to study star-forming regions at greater depth, cloudshine will be widely observed and should be seen as a new high-resolution tool, rather than an inconvenience.

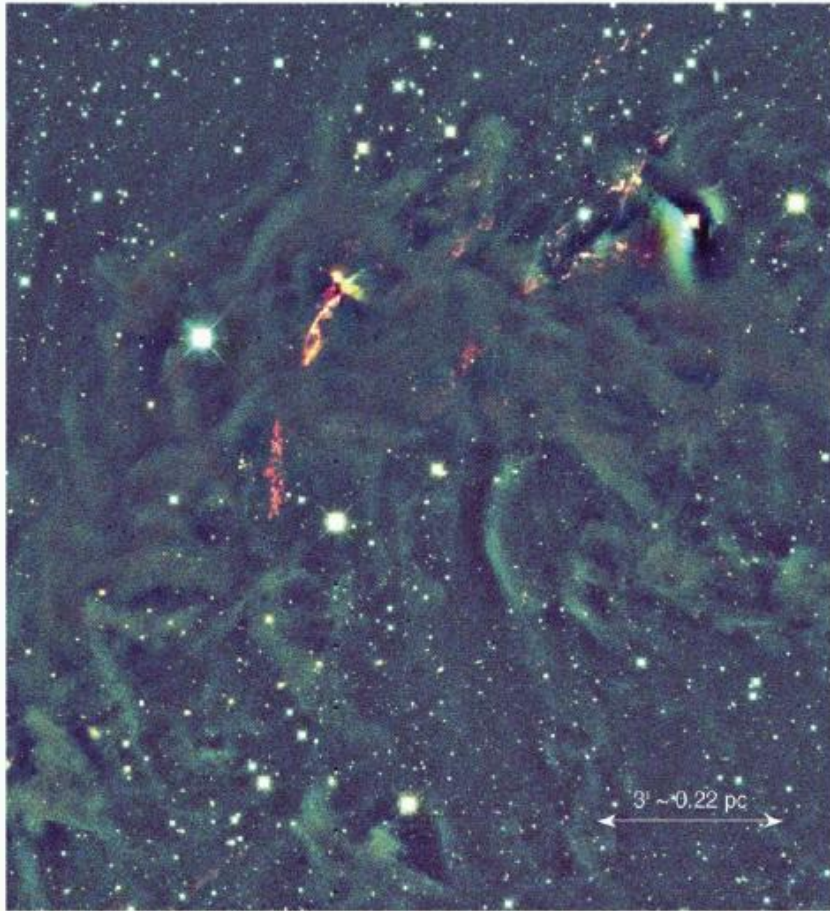


FIG. 1.—L1448 in false color. Component images have been weighted according to their flux in units of  $\text{MJy sr}^{-1}$ .  $J$  is blue,  $H$  is green, and  $K_s$  is red. Outflows from young stars glow red, while a small fan-shaped reflection nebula in the upper right is blue-green. Cloudshine, in contrast, is shown here as a muted glow with green edges. Dark features around extended bright objects (such as the reflection nebula) are the result of self-sky subtraction.

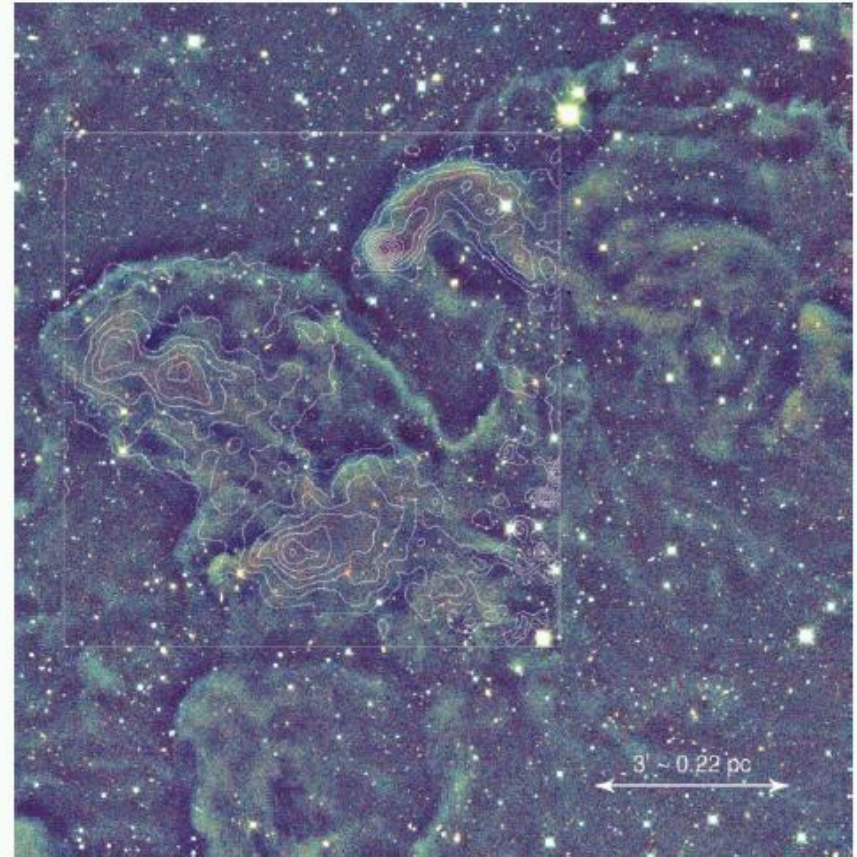


FIG. 2.—L1451 in false color. Again, each component image has been scaled to the same flux scale in units of  $\text{MJy sr}^{-1}$ ; and  $J$  is blue,  $H$  is green, and  $K_s$  is red. A smaller map of 1.2 mm dust emission contours from COMPLETE (M. Tafalla 2006, in preparation) has been overlaid, showing that the color of cloudshine is a tracer of density. Redder regions have high dust continuum flux, and the edges of cloudshine match the edges of the dust emission. Dark edges around bright features (particularly noticeable along the northern edges) are the result of self-sky subtraction.

# Conclusion

The centers of massive clusters is all about

**RESOLUTION, RESOLUTION, RESOLUTION !!!**

we need near-IR AO simulations

with „cloud-shine“ (Foster & Goodman 2006)